AIMS Mathematics, 10(3): 6694–6718.
DOI: 10.3934/math.2025306
Received: 14 January 2025
Revised: 16 March 2025
Accepted: 20 March 2025
Published: 25 March 2025

https://www.aimspress.com/journal/Math

Research article

Blockchain asset portfolio optimization with proportional and fixed transaction fees

Liyuan Zhang, Limian Ci, Yonghong Wu and Benchawan Wiwatanapataphee*

School of Electrical Engineering, Computing & Mathematical Science, Curtin University, Kent Street, Perth 6102, WA, Australia

* **Correspondence:** Email: b.wiwatanapataphee@curtin.edu.au; Tel: +61892662405.

Abstract: The rapid expansion of blockchain technology has created both opportunities and challenges in financial markets, particularly in the investment of blockchain-based real estate tokens. Unlike traditional financial assets, these investments exhibit high volatility, decentralized trading mechanisms, and complex transaction fee structures, all of which significantly influence portfolio management strategies. This study tackled the core issue of portfolio optimization in blockchain asset markets by incorporating both proportional and fixed transaction costs, factors often overlooked in conventional models. To address this, we proposed a multi-period investment optimization framework that leveraged Lagrange multipliers and dynamic programming to determine optimal asset allocation. A key feature of our model was its ability to define an optimal no-trade region, balancing transaction costs with investment returns under varying fee structures. Through numerical experiments, we analyzed how different levels of transaction costs impacted trading frequency, risk exposure, and portfolio efficiency. Our findings indicated that higher transaction costs expanded the no-trade region, reducing trading frequency, while lower costs encouraged more frequent rebalancing. Additionally, we highlighted the practical benefits of blockchain real estate tokenization, including lower investment barriers, enhanced market liquidity, and seamless cross-border transactions. By providing a robust theoretical and empirical framework, this research offered valuable insights for investors navigating blockchain-based financial markets and contributed to the broader discourse on decentralized finance (DeFi) and tokenized real estate investments.

Keywords: blockchain; asset portfolio optimization; proportional transaction fees; fixed transaction costs; real estate tokenization
Mathematics Subject Classification: 00A72, 00A71, 49M99

1. Introduction and literature review

The traditional investment model mainly relies on portfolio management of financial assets such as stocks, bonds, and futures to achieve asset appreciation and risk control. The mean-variance model proposed by Markowitz in 1952 is one of the cornerstones of traditional portfolio theory [1]. By balancing the expected return and risk of an asset, the author provided investors with a theoretical basis for optimizing an asset portfolio for a given level of risk. Based on this theory, investors can construct diversified portfolios to reduce the impact of fluctuations in a single asset on the overall portfolio, thereby maximizing the risk-adjusted return on their investments while achieving the desired return. Thereafter, Merton [2] further developed the dynamic asset allocation (DAA) theory to extend traditional portfolio optimization to multi-period investment situations, enabling investors to dynamically adjust their asset portfolios over a multi-period timeline in response to changing market conditions.

Traditional investment theory usually assumes that transaction costs do not exist or are negligible in the market, and traditional investment models often rely on financial data and analyst forecasts to reduce information asymmetry and improve investment efficiency [3]. However, in actual financial markets, investors often have to pay certain transaction costs when buying and selling assets, and these costs can affect investors' actual returns and strategy choices [4]. Additionally, ownership structures significantly influence the cost of financial intermediation, indicating that institutional characteristics can materially affect portfolio management strategies and costs in traditional financial markets [5]. In order to solve this problem, Magill and Constantinides [6] first proposed a portfolio model with transaction costs and systematically combined the concept of "No-Trade Region", pointing out that investors do not adjust portfolios frequently because of transaction costs, but allow asset allocations to fluctuate within certain ranges and adjust only when the proportion of assets deviates from those ranges. Later, Boyle and Vorst [7] further incorporated fixed transaction costs into a multi-period investment model and analyzed the optimal rebalancing strategies under various forms of transaction costs. These studies reveal the importance of transaction costs in traditional portfolio management and provide a theoretical basis for portfolio optimization that incorporates cost constraints. However, transaction costs in traditional investment models focus on proportional costs (e.g., commissions in the securities market) [8, 9] or fixed transaction fees [10], and usually only consider the impact of a single form of cost on the investment strategy. With the globalization and complexity of financial markets, particularly in blockchain asset investing, which has emerged in recent years, traditional investment models are not well-equipped to meet the investment challenges of emerging markets.

Blockchain asset investment is an emerging investment model that has gained widespread attention in recent years due to the rapid growth of decentralized finance (DeFi). Blockchain assets, which typically include cryptocurrencies (e.g., Bitcoin, Ether, Ripple (XRP), Litecoin, Cardano, and Polkadot) and various types of tokens (e.g., tokens to be converted from physical assets, governance tokens for decentralized applications, etc.), are significantly different from traditional financial assets [11]. To begin, blockchain asset trading is a decentralized trading mechanism based on a blockchain network that does not rely on a centralized exchange and allows investors to directly trade peer-to-peer on a global scale. Due to the decentralized trading environment, blockchain transactions are usually not subject to a single regulator, and investors' trading autonomy and privacy are greatly enhanced [12].

Blockchain assets are highly volatile and have complex price dynamics, which are fundamentally different from assets such as stocks and bonds in traditional financial markets. Price fluctuations in the blockchain market are often affected by a variety of factors, such as market sentiment, project development, government policies and regulations and cybersecurity. The prices of blockchain assets may fluctuate dramatically in a short period of time [13]. This high volatility poses a great challenge to investors' risk management and also makes it difficult for traditional portfolio models to respond effectively [14]. Recent research also points to significant linkages between Bitcoin and green financial assets, crude oil, and emerging equity markets, which further supports the view in our paper about the growing possibility and importance of blockchain assets as an asset allocation tool [15]. To achieve better risk control and return management in the blockchain market, investors need to design more flexible investment strategies and introduce new risk management tools. Most critically, there are complex and varied transaction fee structures in blockchain asset investments. Unlike a single proportional or fixed fee in traditional financial markets, transaction fees for blockchain assets typically consist of two types: pro rata fees (e.g., liquidity fees on decentralized exchanges) and fixed fees (e.g., gas fees paid on on-chain transactions) [16]. Pro rata fees are similar to commission fees in traditional financial markets and are proportional to the amount of the transaction [17]. Fixed fees, on the other hand, are fees that are paid for every transaction and are independent of the amount of the transaction, such as a gas fee of a certain amount that is paid when a transaction is made on the Ether chain, regardless of the amount of the transaction. As transaction fees (e.g., gas fees) on blockchain networks are closely related to the busyness of the network and the specific design of the blockchain technology protocol, this makes it possible for transaction fees to fluctuate drastically over time, which can have a significant impact on the actual cost of transactions for investors [18].

Since 2019, the rapid development of blockchain technology has prompted more and more traditional industries to apply the technology for the innovation and optimization of business models [19]. Among them, the real estate industry, as a typical traditional capital-intensive industry, has gradually combined with blockchain technology, giving rise to the emerging investment method of 'blockchain real estate tokenization'. By tokenizing real estate assets, investors are able to hold and trade shares of real estate in the form of digital tokens [20]. Specifically, a real estate project can be divided into a number of shares, each of which corresponds to a separate token, and investors can own a portion of the real estate by purchasing some of these tokens, just as they would buy some stocks. This approach not only reduces the capital requirements for real estate investment, enabling retail investors to participate, but also enhances the liquidity and divisibility of real estate assets. In addition, this tokenization approach enables easier and more transparent cross-border investments globally, as tokens can be freely circulated, traded and transferred on the blockchain network [21].

In traditional portfolio analyzes that include proportional transaction costs, many studies have explored the far-reaching impact of proportional transaction costs on investment strategies and portfolio selection. For example, many scholars have investigated the optimal investment strategy under a single proportional transaction cost and concluded that the existence of transaction costs significantly reduces the trading frequency of investors, which affects the rebalancing decision of investment portfolios [22–24]. In addition, by introducing the concept of 'No-Trade Region', the related literature systematically analyzes why, under a certain proportion of transaction costs, investors would choose to keep the existing asset allocation unchanged within a specific interval in order to avoid unnecessary trading expenditures [25, 26]. These studies not only successfully explain the constraining effect of

transaction costs on investment behavior, but also provide a theoretical basis for understanding how proportional transaction costs change the optimal asset allocation. However, most of the literature focuses mainly on the impact of a single proportional transaction cost and ignores the role of fixed transaction costs in real market environments. Fixed transaction costs are fixed fees that need to be paid per transaction, regardless of the transaction amount, and they are particularly significant for small transactions, which may significantly alter investors' trading strategies and rebalancing decisions [27].

Fixed transaction costs have been incorporated into multi-period investment models and analyzed for their impact on optimal investment strategies. However, much of the existing literature assumes that proportional transaction fees are symmetric and fixed transaction fees are the same or converge to 0, meaning that the same percentage of transaction costs applies to both buying and selling assets [28,29]. This assumption could simplify theoretical models, but it is not always valid in real-world scenarios. Particularly in blockchain platforms, the proportional transaction fees for buying and selling are usually asymmetric due to the peculiarities of the decentralized trading environment. For example, on a decentralized exchange (DEX), an investor may have to pay a proportional liquidity fee when buying an asset and a higher proportional fee when selling. At the same time, fixed fees (e.g., gas fees) per on-chain transaction may also vary significantly across time [30]. In this case, models that only consider a single form of fee or assume fee symmetry will not be able to accurately portray the complex trading environment in the blockchain market, nor can they effectively guide investors to make optimal decisions in that environment.

Various optimization methods have been developed for portfolio optimization, such as the "Minimax and biobjective portfolio selection based on collaborative neurodynamic optimization" [31], and the "Numerical Solution of Dynamic Portfolio Optimization with Transaction Costs" [32]. Based on these studies, this paper proposes a multi-period portfolio optimization model capable of handling both proportional and fixed transaction fees based on the characteristics of blockchain real estate token investment and further considers the case of asymmetric buying and selling fees. The model extends the existing portfolio theory by introducing different forms of transaction costs, such as proportional costs at the time of buying, proportional costs at the time of selling, and fixed transaction costs in different scenarios so that it can more accurately describe the interactions of different forms of costs in the blockchain market and their impact on investor behaviors. The structure of this paper is as follows: Section 2 constructs a multi-period portfolio optimization model and employs the Lagrange multiplier method and dynamic programming techniques to derive the optimal asset allocation strategy under a given expected return constraint. Section 2 derives the optimal trading strategy for the objective function within a no-trade region and identifies the optimal buying and selling points for each trading period to minimize the variance in final wealth. Section 3 analyzes the optimal equilibrium between risk and return under different trading cost conditions by constructing the efficient frontier and gives an explicit solution for the optimal strategy. Section 4 shows some numerical experiments, followed by the main conclusions in Section 5. In Section 6, we discuss limitations and future work based on our research.

Based on the process described above, our main contributions are as follows: First, we propose an innovative multi-period investment optimization framework specifically designed for blockchain asset markets. This framework integrates Lagrange multipliers and dynamic programming to optimize asset allocation strategies while accounting for transaction costs. Second, we explicitly incorporate both proportional and fixed transaction costs into our model, which are often overlooked in traditional

portfolio optimization frameworks. By defining an optimal no-trade region, our approach effectively balances transaction costs with investment returns, leading to more efficient investment decision-making. Furthermore, through numerical experiments, we analyze how different levels of transaction costs impact trading frequency, risk exposure, and portfolio efficiency. Our results reveal that higher transaction costs widen the no-trade region, reducing trading frequency, while lower transaction costs encourage more frequent portfolio rebalancing. Additionally, our study highlights the practical significance of blockchain-based real estate tokenization in lowering investment barriers, increasing market liquidity, and facilitating seamless cross-border transactions. This research contributes to blockchain asset management, DeFi, and tokenized real estate investments, providing a robust theoretical and empirical foundation for future studies in these emerging fields.

2. The model

Consider a financial market that includes two types of trading securities: Risk-free asset and risky real estate token asset (RET asset). Investors engage in sequential investment decisions over $T + 1$ trading periods within a finite planning horizon, denoted by $t = 0, 1, \ldots, T$. Let C_t^0 represent the price of the risk-free asset, and C_t indicate the price of the risky asset at time t. For $t = 0, 1, \ldots, T - 1$, the total returns on the risk-free asset and the risky asset are expressed as $r_0 = \frac{C_{t+1}^0}{C_t^0}$ and $r_t = \frac{C_{t+1}}{C_t}$, respectively. In this context, r_0 is assumed to be a constant, while r_t is treated as a random variable.

Assume that at the initial time $t = 0$, an investor holds a portfolio consisting of h_0^0 dollars in the risk-free asset and h_0 dollars in the risky asset. During each trading period $t = 0, 1, \ldots, T - 1$, the investor makes portfolio adjustments to maximize the expected utility of terminal wealth. Let h_t^0 and h_t denote the amounts of the risk-free and risky assets in the portfolio before trading at time t. The proportional transaction cost for trading the risky asset is $g(\theta)$, and there is a fixed transaction cost F. The variable x_t represents the investor's decision on the amount of the risky asset to trade at time t. The corresponding relationships are as follows:

$$z_t^0 = h_t^0 - x_t - g(\theta) \cdot |x_t| - FH(x_t), \tag{2.1}$$

$$z_t = h_t + x_t, \tag{2.2}$$

where α and β are proportional transaction costs for $x_t > 0$ and $x_t < 0$ respectively, and F_1 and F_2 are fixed transaction costs for $x_t > 0$ and $x_t < 0$ respectively. $z_t^0 \geq 0$ represents the amount of the risk-free asset in dollars, and $z_t \geq 0$ represents the amount of the risky token asset in dollars at time t after trading. The function $H(\cdot)$ is defined as an indicator function by

$$H(x_t) = \begin{cases} 0, & \text{if } x_t = 0, \\ 1, & \text{otherwise.} \end{cases}$$

Thus, the portfolio values before trading at time $t + 1$ are given by

$$h_{t+1}^0 = z_t^0 r_0 = \left(h_t^0 - x_t - g(\theta) \cdot |x_t| - FH(x_t)\right) r_0, \tag{2.3}$$

$$h_{t+1} = z_t r_t = (h_t + x_t) r_t. \tag{2.4}$$

The feasible investment strategies are described by (2.3) and (2.4). The investor aims to minimize the variance of the terminal wealth expressed as

$$VarW(T) \equiv E\left[(W(T) - E[W(T)])^2\right] = E\left[(W(T) - G)^2\right],$$

where $E[W(T)] = G$ represents a target mean wealth, with $G \geq W(0)e^{rT}$. Consequently, the investor's objective is formulated as a mean-variance (GV) portfolio optimization problem:

$$\begin{aligned} &\min E[W(T) - G]^2 \\ &\text{subject to} \quad \begin{cases} EW(T) = G, \\ (h_t^0, h_t, x_t) \text{ satisfy (2.3) and (2.4)}, \\ t = 0, 1, \ldots, T-1, \end{cases} \end{aligned} \tag{2.5}$$

where $W(T) = h_T^0 + h_T$ means the total of all the assets, considering the initial portfolio (h_0^0, h_0).

It is evident that the problem in (2.5) represents a dynamic quadratic convex optimization task. To derive the optimal strategy that meets the constraint $E[W(T)] = G$, a Lagrange multiplier $2\lambda \in \mathbb{R}$ is introduced. This leads to the formulation of a new cost function, namely:

$$\hat{Q}(\lambda) = E\left[(W(T) - G)^2 + 2\lambda(W(T) - G)\right] = E\left[(W(T) - (G - \lambda))^2\right] - \lambda^2.$$

By setting $\gamma = G - \lambda$, the problem described in (2.5) can be addressed by the following optimization problem:

$$\begin{aligned} &\min \bar{Q}(\gamma) = E[W(T) - \gamma]^2 - (G - \gamma)^2 \\ &\text{subject to} \quad \begin{cases} (h_t^0, h_t, x_t) \text{ satisfy (2.3) and (2.4)}, \\ t = 0, 1, \ldots, T-1. \end{cases} \end{aligned} \tag{2.6}$$

The transition from (2.5) to (2.6) utilizes the Lagrange duality theorem, which reformulates the original problem (2.5) within a dual framework, leading to the optimization problem in (2.6) with the objective function $\bar{Q}(\gamma)$. Therefore,

$$\min \text{Var } W(T) = \max_{\lambda \in \mathbb{R}} \min \hat{Q}(\lambda) = \max_{\gamma \in \mathbb{R}} \min \bar{Q}(\gamma). \tag{2.7}$$

For a fixed constant γ, it is apparent that the optimization problem presented in (2.7) can be directly interpreted as equivalent to the following problem:

$$\begin{aligned} &\min E[h_T^0 + h_T - \gamma]^2 \\ &\text{subject to} \quad \begin{cases} (h_t^0, h_t, x_t) \text{ satisfy (2.3) and (2.4)}, \\ t = 0, 1, \ldots, T-1. \end{cases} \end{aligned} \tag{2.8}$$

Through the application of the Lagrange multiplier and duality theory, the original problem (2.6) is transformed into the problem presented in (2.8), which is amenable to solution via a dynamic programming technique. In [33], the terminal utility function U is assumed to exhibit specific characteristics: it is concave, indicating diminishing marginal utility with increasing wealth; it is

homogeneous, meaning that scaling wealth by a factor leads to the utility being scaled by a power of that factor, represented by α; and it is differentiable, which implies that the function is smooth and has a well-defined derivative. Under these assumptions, the following transformations are formulated:

$$\begin{aligned} \bar{h}_T^0 &= h_T^0 - \gamma \\ \bar{h}_t^0 &= h_t^0 - \gamma \cdot \left(\frac{1}{r_0}\right)^{T-t}, \quad t = 0, 1, \ldots, T-1. \end{aligned} \tag{2.9}$$

Consequently, problem (2.8) can be reformulated as

$$\begin{aligned} &\min E[U(\bar{h}_T^0, h_T)] = E[\bar{h}_T^0, h_T]^2 \\ &\text{subject to} \quad \begin{cases} \bar{h}_{t+1}^0 = \left(h_t^0 - x_t - g(\theta) \cdot |x_t| - FH(x_t)\right) r_0 \\ h_{t+1} = (h_t + x_t) r_t \\ t = 0, 1, \ldots, T-1. \end{cases} \end{aligned} \tag{2.10}$$

Defining the indirect utility function V_t is a key step in applying the dynamic programming technique. The expression for V_t is as follows:

$$V_t(\bar{h}_t^0, h_t) = \begin{cases} U(\bar{h}_T^0, h_T), & t = T, \\ \min\limits_{x_t} E_{r_t} V_{t+1}(\bar{h}_{t+1}^0, h_{t+1}), & t = 0, 1, \ldots, T-1. \end{cases} \tag{2.11}$$

The expectation E_{r_t} is the conditional expectation of the future asset return r_t, given the current state variables ($\bar{h}_t^0$ and h_t) at time t.

3. Optimal strategy

In order to solve the problem (2.10), this section describes the detailed steps. The derivation of the method is based on the core theorem in [33].

Let

$$\Phi_t(x_t, \bar{h}_t^0, h_t) = E_{r_t} V_{t+1}(\bar{h}_{t+1}^0, h_{t+1}). \tag{3.1}$$

The no-trade interval is defined as the area where the expected value cannot be improved by buying or selling the risky asset within any portfolio, and the following definition is provided.

Definition 3.1. If the set of portfolios Φ_t satisfies

$$\Phi_t = \{(\bar{h}_t^0, h_t) \mid \phi_t(x_t, \bar{h}_t^0, h_t) \geq \phi_t(0, \bar{h}_t^0, h_t), \text{ for all } x_t\}, \tag{3.2}$$

then Φ_t is termed the no-trade interval at time t.

In [33], if variables m_t and n_t satisfy $0 < m_t \leq n_t < \infty$, then the no-trade interval can be expressed as

$$\Phi_t = \left\{(\bar{h}_t^0, h_t) \mid m_t \leq \frac{h_t}{\bar{h}_t^0} \leq n_t\right\},$$

where

$$m_t = \min\left\{h_t \mid \frac{\partial^+\phi_t(0,1,h_t)}{\partial x_t} = 0, h_t \geq 0\right\},$$
$$n_t = \max\left\{h_t \mid \frac{\partial^-\phi_t(0,1,h_t)}{\partial x_t} = 0, h_t \geq 0\right\}.$$

Here, $\frac{\partial^+\phi_t}{\partial x_t}$ and $\frac{\partial^-\phi_t}{\partial x_t}$ represent the right and left derivatives of Φ_t, respectively. Based on this bound, the optimal investment strategy outside the no-trade interval is inscribed in Theorem 2.

Theorem 2. *If* $m_t > \dfrac{h_t}{\bar{h}_t^0}$, *then*

$$\min_{x_t} \phi_t(x_t, \bar{h}_t^0, h_t) = \phi_t(x_t^+, \bar{h}_t^0, h_t) = \phi_t(0, z_t^{0+}, z_t^+) \tag{3.3}$$

where

$$\begin{aligned} x_t^+ &= \frac{(\bar{h}_t^0 - F_1)m_t - h_t}{1 + (1+\alpha)m_t} \\ z_t^{0+} &= \bar{h}_t^0 - (1+\alpha)x_t^+ - F_1 \\ z_t^+ &= h_t + x_t^+, \end{aligned} \tag{3.4}$$

with $(z_t^{0+}, z_t^+) \in \Phi_t$ *and* $\dfrac{z_t^+}{z_t^{0+}} = m_t$.

If $n_t < \dfrac{x_t}{\bar{x}_t^0}$, *then*

$$\min_{x_t} \phi_t(x_t, \bar{h}_t^0, h_t) = \phi_t(x_t^-, \bar{h}_t^0, h_t) = \phi_t(0, z_t^{0-}, z_t^-), \tag{3.5}$$

where

$$\begin{aligned} x_t^- &= \frac{(\bar{h}_t^0 - F_2)n_t - h_t}{1 + (1-\beta)n_t} \\ z_t^{0-} &= \bar{h}_t^0 - (1-\beta)x_t^- - F_2 \\ z_t^- &= h_t + x_t^-, \end{aligned} \tag{3.6}$$

with $(z_t^{0-}, z_t^-) \in \Phi_t$ *and* $\frac{z_t^-}{z_t^{0-}} = n_t$.

Proof. **Scenario 1.** $m_t > \dfrac{h_t}{\bar{h}_t^0}$.

If $m_t < \infty$, for $x_t^+ > 0$,

$$\begin{aligned} &\frac{\partial \phi_t(x_t^+, \bar{h}_t^0, h_t)}{\partial x_t} \\ &= -r^0(1+\alpha)E_{r_t}\frac{\partial V_{t+1}((\bar{h}_t^0 - (1+\alpha)x_t^+ - F_1 H(x_t^+))r^0, (h_t + x_t^+)r_t)}{\partial \bar{h}_{t+1}^0} \end{aligned}$$

$$
\begin{aligned}
&+ E_{r_t} r_t \frac{\partial V_{t+1}((\bar{h}_t^0 - (1+\alpha)x_t^+ - F_1 H(x_t^+))r^0, (h_t + x_t^+)r_t)}{\partial h_{t+1}} \\
&= (\bar{h}_t^0 - (1+\alpha)x_t^+ - F_1) \cdot \left(-r^0(1+\alpha) E_{r_t} \frac{\partial V_{t+1}(r^0, m_t r_t)}{\partial \bar{h}_{t+1}^0} + E_{r_t} r_t \frac{\partial V_{t+1}(r^0, m_t r_t)}{\partial h_{t+1}} \right) \\
&= (\bar{h}_t^0 - (1+\alpha)x_t^+ - F_1) \cdot \frac{\partial \phi_t^+(0, 1, m_t)}{\partial x_t}.
\end{aligned}
$$

By Definition 3.1, we get $\dfrac{\partial^+ \phi_t(0, 1, m_t)}{\partial x_t} = 0$, therefore,

$$
\frac{\partial \phi_t(x_t^+, \bar{h}_t^0, h_t)}{\partial x_t} = 0.
$$

Hence, x_t^+ is a minimum point.

If $m_t = \infty$, since the function ϕ_t is a nonincreasing function, the right endpoint x_t^+ is at the far right of its domain of definition and is therefore the point of minimum value of ϕ_t. Hence, x_t^+ is the minimum point. □

Proof. **Scenario 2.** $n_t < \dfrac{h_t}{\bar{h}_t^0}$.

Similar to scenario 1, if $n_t < \infty$, for $x_t^- < 0$,

$$
\begin{aligned}
&\frac{\partial \phi_t(x_t^-, \bar{h}_t^0, h_t)}{\partial x_t} \\
&= -r^0(1-\beta) E_{r_t} \frac{\partial V_{t+1}((\bar{h}_t^0 - (1-\beta)x_t^- - F_1 H(x_t^-))r^0, (h_t + x_t^-)r_t)}{\partial \bar{h}_{t+1}^0} \\
&\quad + E_{r_t} r_t \frac{\partial V_{t+1}((\bar{h}_t^0 - (1+\beta)x_t^- - F_1 H(x_t^-))r^0, (h_t + x_t^-)r_t)}{\partial h_{t+1}} \\
&= (\bar{h}_t^0 - (1-\beta)x_t^- - F_1) \cdot \left(-r^0(1-\beta) E_{r_t} \frac{\partial V_{t+1}(r^0, m_t r_t)}{\partial \bar{h}_{t+1}^0} + E_{r_t} r_t \frac{\partial V_{t+1}(r^0, m_t r_t)}{\partial h_{t+1}} \right) \\
&= (\bar{h}_t^0 - (1-\beta)x_t^- - F_1) \cdot \frac{\partial \phi_t^-(0, 1, m_t)}{\partial x_t}.
\end{aligned}
$$

Due to $\dfrac{\partial \phi_t^-(0, 1, m_t)}{\partial x_t} = 0$ in Definition 3.1, one gets

$$
\frac{\partial \phi_t(x_t^-, \bar{h}_t^0, h_t)}{\partial x_t} = 0.
$$

Consequently, x_t^- is a minimum point.

If $n_t = \infty$ and x_t^- is still a minimum point, science the function ϕ_t is a nonincreasing function, and x_t^- is the right endpoint of its domain. □

Now, the value of m_t, n_t, and the value function $V_t(\bar{h}_t^0, h_t)$ are shown. To begin with, we introduce the definition of the indirect utility function.

Definition 3.3. The function Q is a piecewise linear utility function composed of segments, each linearly dependent on U. These segments are shaped by the probabilities of various outcomes $\Pr(p_i)$, where $\{p_i; i = 1, \ldots, I\}$ represents the underlying probability space, describing all possible future scenarios. For each interval defined by the sequence s_j $(j = 1, \ldots, q)$, the function Q is expressed in terms of nonnegative constants μ_{ij} and ρ_{ij}. Specifically, within each interval $s_j \leq \frac{h}{h^0} \leq s_{j+1}$, Q can be written as:

$$Q(h^0, h) = \sum_{i=1}^{I} U(\mu_{ij} h^0, \rho_{ij} h) \Pr(p_i). \tag{3.7}$$

Here, p_i represents different scenarios in the probability space, and $\Pr(p_i)$ is the probability associated with each scenario. The constants μ_{ij} and ρ_{ij} define the linear relationship within each interval, determining how Q changes as the ratio $\frac{h}{h^0}$ varies across the intervals s_j.

Suppose the value function $V_t(\bar{h}_t^0, h_t)$ is a piecewise linear utility function with respect to U. This means that the value function can be approximated by a linear function in each interval, thus simplifying the solution of dynamic programming problems. Taking time t as the time point, all possible results for r_t at time t are denoted by $\{r_t^w; w = 1, \ldots, W\}$, and the set of all possible future paths $(r_{t+1}, r_{t+2}, \ldots, r_T)$ from moment $t + 1$ to moment T are denoted by $\{p_i\}$, and the paths are defined based on a tree structure of a node at time t+1. Then, all the paths that start at time t can be denoted as $\{(r_t^w, p_i)\}$. Thus, the utility function Q_t can be computed recursively starting at time $t = T$.

At $t = T$ and $x_t = 0$,

$$V_T(\bar{h}_T^0, h_T) = U(\bar{h}_T^0, h_T) = (\bar{h}_T^0 + h_T)^2. \tag{3.8}$$

Assume that

$$\begin{aligned} V_{t+1}(\bar{h}_{t+1}^0, h_{t+1}) &= \sum_{i=1}^{I} U(\mu_{ij} \bar{h}_{t+1}^0, \rho_{ij} h_{t+1}) \Pr(p_i) \\ &= \sum_{i=1}^{I} (\mu_{ij} \bar{h}_{t+1}^0 + \rho_{ij} h_{t+1})^2 \Pr(p_i) \\ s_j \leq \frac{h_{t+1}}{\bar{h}_{t+1}^0} &\leq s_{j+1}, \quad j = 0, 1, \ldots, q \\ s_0 = 0, \quad s_{s+1} &= \infty. \end{aligned} \tag{3.9}$$

Then

$$\begin{aligned} \phi_t(0, \bar{h}_t^0, h_t) &= E_{r_t} V_{t+1}(\bar{h}_t^0 r^0, h_t r_t) \\ &= \sum_{w=1}^{W} \sum_{i=1}^{I} U(\mu_{ij} r^0 \bar{h}_t^0, \rho_{ij} r_t^w h_t) \Pr\{(r_t^w, p_i)\} \end{aligned}$$

$$= \sum_{w=1}^{W} \sum_{i=1}^{I} (\mu_{ij} r^0 \bar{h}_t^0 + \rho_{ij} r_t^w h_t)^2 \Pr\{(r_t^w, p_i)\}. \tag{3.10}$$

Let $\tilde{\mu}_{ij} = \mu_{ij} r^0$, $\tilde{\rho}_{ij} = \rho_{ij} r_t^w$.

When $x_t \geq 0$,

$$\phi_t(x_t, \bar{h}_t^0, h_t) = \sum_{w=1}^{W} \sum_{i=1}^{I} \left\{ \tilde{\mu}_{ij} \left[\bar{h}_t^0 - (1+\alpha) x_t \right] + \tilde{\rho}_{ij} [h_t + x_t] \right\}^2 \Pr\{(r_t^w, p_i)\}. \tag{3.11}$$

When $x_t \leq 0$,

$$\phi_t(x_t, \bar{h}_t^0, h_t) = \sum_{w=1}^{W} \sum_{i=1}^{I} \left\{ \tilde{\mu}_{ij} \left[\bar{h}_t^0 - (1-\beta) x_t \right] + \tilde{\rho}_{ij} [h_t + x_t] \right\}^2 \Pr\{(r_t^w, p_i)\}. \tag{3.12}$$

Hence, m_t is a solution of the equations

$$\sum_{w=1}^{W} \sum_{i=1}^{I} (\tilde{\mu}_{ij} + \tilde{\rho}_{ij} m_t)[\tilde{\rho}_{ij} - (1+\alpha)\tilde{\mu}_{ij}] \Pr\{(r_t^w, p_i)\} = 0 \tag{3.13}$$

$$\tilde{s}_j \leq m_t < \tilde{s}_{j+1}, \quad j = 0, 1, 2, \ldots$$

and n_t is a solution of the equations

$$\sum_{w=1}^{W} \sum_{i=1}^{I} (\tilde{\mu}_{ij} + \tilde{\rho}_{ij} n_t)[\tilde{\rho}_{ij} - (1-\beta)\tilde{\mu}_{ij}] \Pr\{(r_t^w, p_i)\} = 0 \tag{3.14}$$

$$\tilde{s}_j \leq n_t < \tilde{s}_{j+1}, \quad j = 0, 1, 2, \ldots$$

To facilitate the optimization of the portfolio in a multi-period model, the indirect utility function is rearranged. All combinations $\left(\frac{r^0}{r_t^w}\right) s_j$, $w = 1, \ldots, W$, $j = 0, 1, \ldots, q$, are sorted in ascending order, and then relabeled as $\tilde{s}_l$ based on their magnitude.
For $z = 1, ..., I$,

$$\tilde{\mu}_{zl} = \mu_{zj} r^0, \quad \tilde{\rho}_{zl} = \rho_{zj} r_t^1,$$

where $\left(\frac{r^0}{r_t^1}\right) s_j \leq \tilde{s}_l \leq \tilde{s}_{l+1} \leq \left(\frac{r^0}{r_t^1}\right) s_{j+1}$.

For $z = I, ..., 2I$,

$$\tilde{\mu}_{zl} = \mu_{z-I,j} r^0, \quad \tilde{\rho}_{zl} = \rho_{z-I,j} r_t^2,$$

where $\left(\frac{r^0}{r_t^2}\right) s_j \leq \tilde{s}_l \leq \tilde{s}_{l+1} \leq \left(\frac{r^0}{r_t^2}\right) s_{j+1}$.

This process continues similarly for all subsequent combinations. Finally, for $z = (W-1)I+1, ..., WI$, this pattern continues with

$$\tilde{\mu}_{zl} = \mu_{z-(W-1)I,j} r^0, \quad \tilde{\rho}_{zl} = \rho_{z-(W-1)I,j} r_t^W,$$

where the range satisfies $\left(\frac{r^0}{r_t^W}\right) s_j \leq \tilde{s}_l \leq \tilde{s}_{l+1} \leq \left(\frac{r^0}{r_t^W}\right) s_{j+1}$. This iterative process ensures that all combinations are systematically labeled and ranked by magnitude, enabling efficient optimization of the portfolio's multi-period performance.

Building upon the definitions and systematic process outlined above, we then transform z and l back to i to simplify and make the formula more concise and clear. The resulting formulation is expressed as

$$\begin{aligned} \phi_t(0, \bar{h}_t^0, h_t) &= \sum_{w=1}^{W} \sum_{i=1}^{I} (\tilde{\mu}_{ij} \bar{h}_t^0 + \tilde{\rho}_{ij} h_t)^2 \Pr\{(r_t^w, p_i)\} \\ \tilde{s}_j &\leq \frac{h_t}{\bar{h}_t^0} \leq \tilde{s}_{j+1}. \end{aligned} \tag{3.15}$$

According to Theorem 2, the value function can be written as

$$V_t(\bar{h}_t^0, h_t) = \begin{cases} \phi_t(0, z_t^{0+}, z_t^+), & \frac{h_t}{\bar{h}_t^0} < m_t, \\ \phi_t(0, \bar{h}_t^0, h_t), & m_t \leq \frac{h_t}{\bar{h}_t^0} \leq n_t, \\ \phi_t(0, z_t^{0-}, z_t^-), & \frac{h_t}{\bar{h}_t^0} > n_t. \end{cases} \tag{3.16}$$

Suppose that

$$\tilde{s}_{j_1} < m_t \leq \cdots < \tilde{s}_{j_2} \leq n_t < \cdots$$

Let

$$\bar{s}_0 = 0, \quad \bar{s}_1 = m_t, \quad \bar{s}_2 = \tilde{s}_{j_1}, \quad \cdots, \quad \bar{s}_{j_2-j_1+2} = n_t, \quad \bar{s}_{j_2-j_1+3} = \infty \tag{3.17}$$

and

$$\begin{aligned} \bar{\mu}_{i0} &= \frac{\tilde{\mu}_{i,j_1} + m_t \tilde{\rho}_{i,j_1}}{1 + (1 + g(\theta)) m_t}, \quad \bar{\rho}_{i0} = (1 + g(\theta)) \bar{\mu}_{i0} \\ \bar{\mu}_{ij} &= \tilde{\mu}_{i,j_1+j-1}, \quad \bar{\rho}_{ij} = \tilde{\rho}_{i,j_1+j-1}, \quad j = 1, 2, \ldots, j_2 - j_1 + 1 \\ \bar{\mu}_{i,j_2-j_1+2} &= \frac{\tilde{\mu}_{i,j_2} + n_t \tilde{\rho}_{i,j_2}}{1 + (1 - g(\theta)) n_t}, \quad \bar{\rho}_{i,j_2-j_1+2} = (1 - g(\theta)) \bar{\mu}_{i,j_2-j_1+2}. \end{aligned}$$

Then,

$$V_t(\bar{h}_t^0, h_t) = \sum_{w=1}^{W} \sum_{i=1}^{I} (\bar{\mu}_{ij} \bar{h}_t^0 + \bar{\rho}_{ij} h_t)^2 \Pr\{(r_t^w, p_i)\} \tag{3.18}$$

$$\bar{s}_j \le \frac{h_t}{\bar{h}_t^0} \le \bar{s}_{j+1}, \quad j = 0, 1, \ldots.$$

The efficient frontier is an important part of modern portfolio theory. Constructing the efficient frontier can help investors find the optimal portfolio between risk and return. According to (2.5), the relationship between variance and wealth expectancy has been shown. Based on the above derivation, the explicit solution of the value function can be written as:

$$V_t(\bar{h}_t^0, h_t) = \sum_{w=1}^{W}\sum_{i=1}^{I}\left\{\bar{\mu}_{ij}\left[\bar{h}_t^0 - \gamma\cdot\left(\frac{1}{r^0}\right)^{T-t}\right] + \bar{\rho}_{ij}h_t\right\}^2 \Pr\{(r_t^w, p_i)\}, \tag{3.19}$$
$$\bar{s}_j \le \frac{h_t}{\bar{h}_t^0 - \gamma\cdot\left(\frac{1}{r^0}\right)^{T-t}} \le \bar{s}_{j+1}, \quad j = 0, 1, \ldots$$

From (2.7),

$$\min \text{Var } W(T) = \max_{\gamma\in\mathbb{R}} \min \bar{Q}(\gamma) = \max_{\gamma\in\mathbb{R}} Q_t(h_t^0, h_t) - (G-\gamma)^2. \tag{3.20}$$

Therefore, the maximum value of $Q_t(h_t^0, h_t) - (G-\gamma)^2$ in (3.20) is reached at the point γ^*, which satisfies

$$\sum_{w=1}^{W}\sum_{i=1}^{I}\left\{\bar{\mu}_{ij}\left[\bar{h}_t^0 - \gamma^*\cdot\left(\frac{1}{r^0}\right)^{T-t}\right] + \bar{\rho}_{ij}h_t\right\}\bar{\mu}_{ij}\left(\frac{1}{r^0}\right)^{T-t} \Pr\{(r_t^w, p_i)\} + (G-\gamma^*) = 0 \tag{3.21}$$

with leads to

$$\gamma^* = \frac{G - \sum_{w=1}^{W}\sum_{i=1}^{I}(\bar{\mu}_{ij}\bar{h}_t^0 + \bar{\rho}_{ij}h_t)\bar{\mu}_{ij}\left(\frac{1}{r^0}\right)^{T-t} \Pr\{(r_t^w, p_i)\}}{1 - \sum_{w=1}^{W}\sum_{i=1}^{I}\left[\bar{\mu}_{ij}\left(\frac{1}{r^0}\right)^{T-t}\right]^2 \Pr\{(r_t^w, p_i)\}}. \tag{3.22}$$

For the initial moment of investment, i.e., at $t = 0$, given the initial investment condition (h_0^0, h_0), we obtain

$$\gamma^* = \frac{G - \sum_{w=1}^{W}\sum_{i=1}^{I}(\bar{\mu}_{ij}\bar{h}_0^0 + \bar{\rho}_{ij}h_0)\bar{\mu}_{ij}\left(\frac{1}{r^0}\right)^{T} \Pr\{(r_0^w, p_i)\}}{1 - \sum_{w=1}^{W}\sum_{i=1}^{I}\left[\bar{\mu}_{ij}\left(\frac{1}{r^0}\right)^{T}\right]^2 \Pr\{(r_t^w, p_i)\}}. \tag{3.23}$$

Hence,

$$\text{Var } W(T) = V_0(h_0^0, h_0, \gamma^*) - (G-\gamma^*)^2. \tag{3.24}$$

By substituting (3.23) into (3.24), we get the effective boundary.

4. Numerical result

The model analyzes portfolios of risk-free and blockchain-risky assets using a multi-period time-step approach. Assuming a total time horizon of $T = 4$, the parameter $r^0$for the return on the risk-free asset as defined in Section 2 is held constant at 1.0125, which means the asset value increases by 1.25% per annual according to [34], while the proportional and fixed transaction fees of the risky asset (one real estate token) are normally 1.5% to 2% and \$3 to \$5 respectively [35], and the return on one real estate token is predicted based on simulation results from the long short-term memory (LSTM) model as shown in Table 1. Returns are predicted using real estate token data collected from the RealT platform (Figure 1) rather than relying on theoretical assumptions of risky and riskless assets with predetermined up u and down d movements. The LSTM model is trained on historical real estate token return data to capture patterns of return volatility over time. Using the trained LSTM, Monte Carlo simulations are performed to generate various scenario paths over a one-year period, with each time step representing a four-month interval. The predicted data is used to construct a scenario tree that provides a framework for analyzing the potential return distribution of a portfolio and optimizing investment strategies over a one-year time horizon.

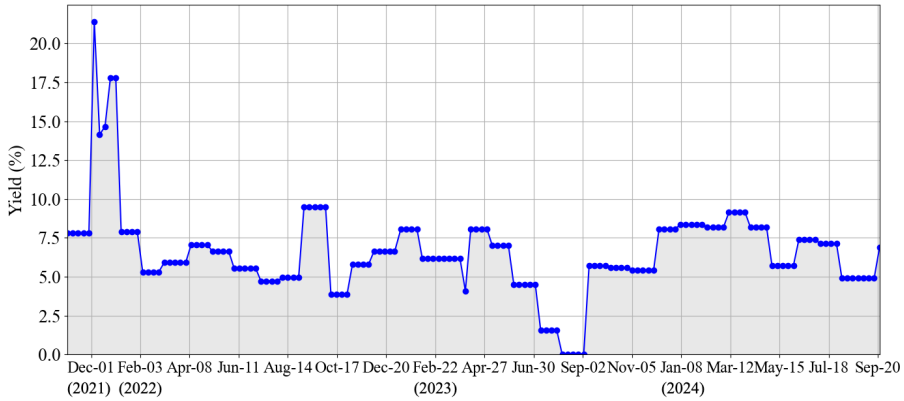

Figure 1. Weekly evolution of annual returns for a typical blockchain real estate token.

Table 1. The risky asset's return and probabilities.

ith Scenario	r_0	r_1	r_2	r_3	Probability
1	1.074	1.339	0.884	0.732	0.260
2	1.074	0.968	0.610	0.655	0.169
3	1.074	1.006	1.004	1.129	0.137
4	1.074	1.133	1.079	0.888	0.100
5	1.074	1.090	0.851	0.950	0.228
6	1.074	1.126	0.997	0.917	0.041
7	1.074	1.040	0.971	0.980	0.050
8	1.074	0.996	0.887	0.953	0.015

According to the scenario tree in Table 1, we can obtain the no-transaction intervals under different prorated commission conditions as shown in Table 2. As shown in Table 2, with the same transaction fee rates for buying and selling, lower prorated fees lead to smaller no-transaction intervals, while higher prorated fees lead to larger no-transaction intervals. Where buy (or sell) has the same proportional transaction fee, a high proportional transaction fee for sale (or buy) leads to a reduction in the corresponding trading behavior of the investor and an increase in the no-transaction interval. Thus, a higher proportional transaction fee for either buying or selling will result in less trading behavior in the corresponding direction, leading investors to prefer to remain in their current holding position. It can also be concluded that when significant asymmetry exists in transaction fees, the width of the no-trade region increases, causing investors to become more conservative in their trading behavior. Conversely, as transaction fees become more symmetric, the no-trade region narrows, prompting investors to adjust their asset allocations more frequently.

Table 2. Results for no-transaction intervals.

	$\alpha = 0.015, \beta = 0.015$	$\alpha = 0.015, \beta = 0.020$	$\alpha = 0.020, \beta = 0.015$	$\alpha = 0.020, \beta = 0.020$
m_0, n_0	0.495, 0.573	0.495, 0.586	0.482, 0.573	0.482, 0.586
m_1, n_1	0.326, 0.373	0.326, 0.381	0.318, 0.373	0.318, 0.381
m_2, n_2	0.209, 0.213	0.209, 0.225	0.193, 0.213	0.193, 0.225
m_3, n_3	0.066, 0.078	0.066, 0.080	0.064, 0.078	0.064, 0.080

Assuming that the initial wealth is 2000 dollars, which aligns with the average weekly salary in Australia, according to the Australian Bureau of Statistics (ABS) [36]. Figure 2 describes the efficient frontier under different trading proportions. When variance = 0, G = 2000, the five boundaries intersect at one end, and at this point, the optimal strategy is to invest in risk-free assets regardless of the transaction fees, which causes the investor to prefer to avoid any risk. As transaction costs increase, the average variance of the efficient frontier decreases, indicating that investors' risk aversion grows. Notably, the efficient frontier without transaction fees ($\alpha = \beta = 0$) lies above all the efficient frontiers that include transaction fees. The effective frontier with the same transaction costs will be higher than the effective frontier with higher transaction costs for buying or selling. The optimal investment decisions for the problem (2.5) are shown in Tables 3–7.

In Table 3, the transaction costs of buying and selling are symmetric ($\alpha = \beta = 0.015$), so investors' trading activities are relatively frequent, especially in multiple scenarios (e.g., Scenarios 1, 2, and 4), and x_t shows a high number of positive and negative trading values, suggesting that investors frequently adjust their positions to achieve the desired asset allocation. The risky asset holdings (h_t) in Table 3 are more volatile and investors buy and sell frequently according to market changes. In Table 4, on the other hand, compared to Table 3, we can see a significant decrease in selling transactions due to the higher cost of selling ($\beta = 0.020$). For instance, in Scenarios 1 and 3, the selling value of x_t is considerably lower compared to that in Table 3, which implies that investors reduce their selling activities because of the high selling cost and choose to hold more risky assets (h_t is relatively high). Table 5, on the other hand, has a higher cost of buying ($\alpha = 0.020$) compared to Table 3, which causes

investors to reduce their buying behavior. Compared to Tables 3 and 4, Table 5 shows relatively lower holdings of risky assets (h_t), especially in Scenarios 2 and 3, where the value of h_t is even lower, suggesting that investors reduce their purchases of risky assets.

In Table 6, the proportional transaction cost is further increased to $\alpha = \beta = 0.020$, which is higher for both buyers and sellers than in that in Table 3. We can see that the trading activity in Table 6 is substantially reduced compared to Table 3, especially in Scenarios 3 and 5, where x_t is almost close to zero, suggesting that in the presence of high transaction costs, investors are more reluctant to trade frequently and tend to maintain their existing positions. The volatility of holding risky assets (h_t) is also significantly lower compared to that in Table 3, reflecting that high costs inhibit investors' reaction to the market. In addition, in Table 6 the no-trading band expands and investors will only trade when the market is volatile enough, so a smaller market changes do not prompt investors to adjust their asset allocation frequently.

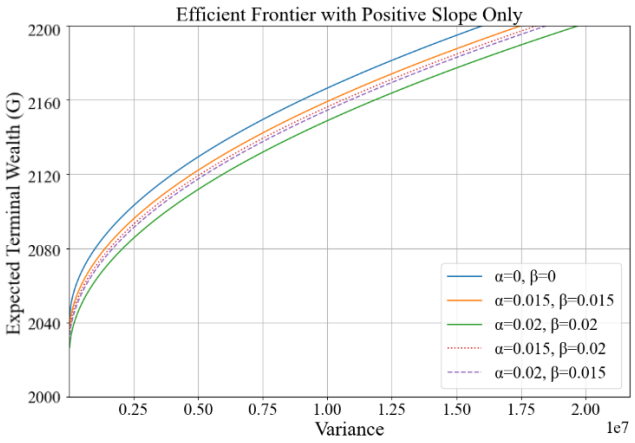

Figure 2. Efficient Frontier with different proportional cost.

Table 3. Numerical results for multiple scenarios with $\alpha = 0.015$ and $\beta = 0.015$.

$\alpha = 0.015, \beta = 0.015, F_1 = 5, F_2 = 3$						
Scenario	**Variable**	**0**	**1**	**2**	**3**	**4**
1	γ_t	0.1853	0.5352	0.2186	0.1485	-
	x_t	831.98	-749.30	-115.30	-178.67	-
	h_t^0	1800.00	962.43	1718.70	1852.14	2050.44
	h_t	200.00	1108.25	480.81	322.97	105.61
2	γ_t	0.1853	0.5352	0.1681	0.1149	-
	x_t	831.98	-749.30	18.17	-89.17	-
	h_t^0	1800.00	962.43	1718.70	1716.45	1823.80
	h_t	200.00	1108.25	347.35	222.90	87.56
3	γ_t	0.1853	0.5352	0.1736	0.1724	-
	x_t	831.98	-749.30	0.00	-226.87	-
	h_t^0	1800.00	962.43	1718.70	1740.19	1985.16
	h_t	200.00	1108.25	361.09	362.44	153.11
4	γ_t	0.1853	0.5352	0.1914	0.1815	-
	x_t	831.98	-749.30	-41.23	-255.89	-
	h_t^0	1800.00	962.43	1718.70	1778.27	2052.66
	h_t	200.00	1108.25	406.75	394.43	122.98
5	γ_t	0.1853	0.5352	0.1855	0.1499	-
	x_t	831.98	-749.30	-25.84	-173.63	-
	h_t^0	1800.00	962.43	1718.70	1762.92	1955.08
	h_t	200.00	1108.25	391.36	310.97	130.55
6	γ_t	0.1853	0.5352	0.1904	0.1702	-
	x_t	831.98	-749.30	-38.56	-225.91	-
	h_t^0	1800.00	962.43	1718.70	1775.60	2020.07
	h_t	200.00	1108.25	404.07	364.25	126.87
7	γ_t	0.1853	0.5352	0.1784	0.1690	-
	x_t	831.98	-749.30	-7.71	-218.85	-
	h_t^0	1800.00	962.43	1718.70	1744.84	1981.88
	h_t	200.00	1108.25	373.23	354.79	133.16
8	γ_t	0.1853	0.5352	0.1723	0.1542	-
	x_t	831.98	-749.30	0.00	-181.64	-
	h_t^0	1800.00	962.43	1718.70	1740.19	1940.06
	h_t	200.00	1108.25	357.68	317.22	129.26

Table 4. Numerical results for multiple scenarios with $\alpha = 0.015$ and $\beta = 0.020$.

$\alpha = 0.015, \beta = 0.020, F_1 = 5, F_2 = 3$						
Scenario	**Variable**	**0**	**1**	**2**	**3**	**4**
1	γ_t	0.1853	0.5471	0.2180	0.1689	-
	x_t	855.39	-776.07	-64.69	-222.02	-
	h_t^0	1800.00	938.36	1717.11	1799.72	2039.48
	h_t	200.00	1133.40	478.63	365.76	105.20
2	γ_t	0.1853	0.5471	0.1676	0.1318	-
	x_t	855.39	-776.07	68.17	-119.57	-
	h_t^0	1800.00	938.36	1717.11	1663.46	1799.85
	h_t	200.00	1133.40	345.77	252.43	86.99
3	γ_t	0.1853	0.5471	0.1731	0.1719	-
	x_t	855.39	-776.07	0.00	-221.94	-
	h_t^0	1800.00	938.36	1717.11	1738.58	1977.49
	h_t	200.00	1133.40	359.45	360.80	156.82
4	γ_t	0.1853	0.5471	0.1908	0.2008	-
	x_t	855.39	-776.07	0.00	-298.07	-
	h_t^0	1800.00	938.36	1717.11	1738.58	2053.04
	h_t	200.00	1133.40	404.90	436.93	123.26
5	γ_t	0.1853	0.5471	0.1849	0.1601	-
	x_t	855.39	-776.07	0.00	-192.59	-
	h_t^0	1800.00	938.36	1717.11	1738.58	1948.37
	h_t	200.00	1133.40	389.58	331.45	131.98
6	γ_t	0.1853	0.5471	0.1898	0.1874	-
	x_t	855.39	-776.07	0.00	-261.99	-
	h_t^0	1800.00	938.36	1717.11	1738.58	2017.23
	h_t	200.00	1133.40	402.24	400.85	127.34
7	γ_t	0.1853	0.5471	0.1779	0.1718	-
	x_t	855.39	-776.07	0.00	-221.77	-
	h_t^0	1800.00	938.36	1717.11	1738.58	1977.32
	h_t	200.00	1133.40	371.54	360.63	136.02
8	γ_t	0.1853	0.5471	0.1717	0.1537	-
	x_t	855.39	-776.07	0.00	-176.92	-
	h_t^0	1800.00	938.36	1717.11	1738.58	1932.82
	h_t	200.00	1133.40	356.06	315.78	132.39

Table 5. Numerical results for multiple scenarios with $\alpha = 0.020$ and $\beta = 0.015$.

$\alpha = 0.020, \beta = 0.015, F_1 = 5, F_2 = 3$						
Scenario	**Variable**	**0**	**1**	**2**	**3**	**4**
1	γ_t	0.1853	0.5363	0.2181	0.1486	-
	x_t	831.98	-750.87	-113.77	-178.50	-
	h_t^0	1800.00	958.21	1716.00	1847.88	2045.96
	h_t	200.00	1108.25	478.71	322.46	105.37
2	γ_t	0.1853	0.5363	0.1677	0.1082	-
	x_t	831.98	-750.87	0.00	-75.52	-
	h_t^0	1800.00	958.21	1716.00	1737.45	1831.46
	h_t	200.00	1108.25	345.83	210.89	88.63
3	γ_t	0.1853	0.5363	0.1732	0.1720	-
	x_t	831.98	-750.87	0.00	-225.49	-
	h_t^0	1800.00	958.21	1716.00	1737.45	1981.02
	h_t	200.00	1108.25	359.51	360.86	152.87
4	γ_t	0.1853	0.5363	0.1909	0.1816	-
	x_t	831.98	-750.87	-40.03	-255.58	-
	h_t^0	1800.00	958.21	1716.00	1774.33	2048.37
	h_t	200.00	1108.25	404.97	393.81	122.71
5	γ_t	0.1853	0.5363	0.1850	0.1500	-
	x_t	831.98	-750.87	-24.70	-173.44	-
	h_t^0	1800.00	958.21	1716.00	1759.05	1950.98
	h_t	200.00	1108.25	389.65	310.49	130.26
6	γ_t	0.1853	0.5363	0.1899	0.1703	-
	x_t	831.98	-750.87	-37.36	-225.65	-
	h_t^0	1800.00	958.21	1716.00	1771.68	2015.83
	h_t	200.00	1108.25	402.31	363.68	126.59
7	γ_t	0.1853	0.5363	0.1780	0.1691	-
	x_t	831.98	-750.87	-6.65	-218.59	-
	h_t^0	1800.00	958.21	1716.00	1741.05	1977.78
	h_t	200.00	1108.25	371.60	354.23	132.87
8	γ_t	0.1853	0.5363	0.1719	0.1538	-
	x_t	831.98	-750.87	0.00	-180.47	-
	h_t^0	1800.00	958.21	1716.00	1737.45	1936.12
	h_t	200.00	1108.25	356.12	315.83	129.06

Table 6. Numerical results for multiple scenarios with $\alpha = 0.020$ and $\beta = 0.020$.

$\alpha = 0.020, \beta = 0.020, F_1 = 5, F_2 = 3$						
Scenario	**Variable**	**0**	**1**	**2**	**3**	**4**
1	γ_t	0.1853	0.5482	0.2175	0.1690	-
	x_t	855.39	-777.72	-63.14	-221.78	-
	h_t^0	1800.00	934.03	1714.36	1795.41	2034.87
	h_t	200.00	1133.40	476.42	365.18	104.95
2	γ_t	0.1853	0.5482	0.1672	0.1079	-
	x_t	855.39	-777.72	0.00	-71.24	-
	h_t^0	1800.00	934.03	1714.36	1735.79	1825.15
	h_t	200.00	1133.40	344.18	209.88	90.77
3	γ_t	0.1853	0.5482	0.1727	0.1714	-
	x_t	855.39	-777.72	0.00	-220.50	-
	h_t^0	1800.00	934.03	1714.36	1735.79	1973.24
	h_t	200.00	1133.40	357.80	359.13	156.57
4	γ_t	0.1853	0.5482	0.1903	0.2004	-
	x_t	855.39	-777.72	0.00	-296.28	-
	h_t^0	1800.00	934.03	1714.36	1735.79	2048.44
	h_t	200.00	1133.40	403.03	434.92	123.06
5	γ_t	0.1853	0.5482	0.1845	0.1597	-
	x_t	855.39	-777.72	0.00	-191.28	-
	h_t^0	1800.00	934.03	1714.36	1735.79	1944.25
	h_t	200.00	1133.40	387.78	329.92	131.77
6	γ_t	0.1853	0.5482	0.1893	0.1869	-
	x_t	855.39	-777.72	0.00	-260.36	-
	h_t^0	1800.00	934.03	1714.36	1735.79	2012.79
	h_t	200.00	1133.40	400.38	399.00	127.14
7	γ_t	0.1853	0.5482	0.1774	0.1714	-
	x_t	855.39	-777.72	0.00	-220.33	-
	h_t^0	1800.00	934.03	1714.36	1735.79	1973.08
	h_t	200.00	1133.40	369.82	358.97	135.80
8	γ_t	0.1853	0.5482	0.1713	0.1533	-
	x_t	855.39	-777.72	0.00	-175.69	-
	h_t^0	1800.00	934.03	1714.36	1735.79	1928.78
	h_t	200.00	1133.40	354.42	314.33	132.18

Table 7. Numerical results for multiple scenarios with $\alpha = 0.020, \beta = 0.020, F_1 = 3, F_2 = 3$.

$\alpha = 0.020, \beta = 0.020, F_1 = 3, F_2 = 3$						
Scenario	**Variable**	**0**	**1**	**2**	**3**	**4**
1	γ_t	0.1853	0.5477	0.2177	0.1690	-
	x_t	855.39	-776.95	-63.86	-221.89	-
	h_t^0	1800.00	936.05	1715.65	1797.43	2037.03
	h_t	200.00	1133.40	477.46	365.45	105.07
2	γ_t	0.1853	0.5477	0.1674	0.1080	-
	x_t	855.39	-776.95	0.00	-71.60	-
	h_t^0	1800.00	936.05	1715.65	1737.09	1826.81
	h_t	200.00	1133.40	344.92	210.34	90.84
3	γ_t	0.1853	0.5477	0.1729	0.1716	-
	x_t	855.39	-776.95	0.00	-221.17	-
	h_t^0	1800.00	936.05	1715.65	1737.09	1975.23
	h_t	200.00	1133.40	358.57	359.91	156.68
4	γ_t	0.1853	0.5477	0.1906	0.2006	-
	x_t	855.39	-776.95	0.00	-297.12	-
	h_t^0	1800.00	936.05	1715.65	1737.09	2050.59
	h_t	200.00	1133.40	403.91	435.86	123.15
5	γ_t	0.1853	0.5477	0.1847	0.1599	-
	x_t	855.39	-776.95	0.00	-191.89	-
	h_t^0	1800.00	936.05	1715.65	1737.09	1946.18
	h_t	200.00	1133.40	388.63	330.63	131.87
6	γ_t	0.1853	0.5477	0.1895	0.1871	-
	x_t	855.39	-776.95	0.00	-261.12	-
	h_t^0	1800.00	936.05	1715.65	1737.09	2014.87
	h_t	200.00	1133.40	401.25	399.86	127.24
7	γ_t	0.1853	0.5477	0.1776	0.1716	-
	x_t	855.39	-776.95	0.00	-221.01	-
	h_t^0	1800.00	936.05	1715.65	1737.09	1975.06
	h_t	200.00	1133.40	370.62	359.75	135.90
8	γ_t	0.1853	0.5477	0.1715	0.1535	-
	x_t	855.39	-776.95	0.00	-176.27	-
	h_t^0	1800.00	936.05	1715.65	1737.09	1930.67
	h_t	200.00	1133.40	355.18	315.01	132.28

The main difference between Tables 6 and 7 lies in the varying fixed trading fees. While α and β remain the same, the fixed transaction fees in Table 6 are $F_1 = 5$ and $F_2 = 3$, while in Table 7

they are $F_1 = 3$ and $F_2 = 3$. As a result, there is slightly more trading activity in Table 7 than in Table 6, e.g., in Scenario 4 and Scenario 5, the x_t selling values in Table 7 are higher, suggesting that the lower fixed transaction fees incentivise some trading behavior. Also, h_t is slightly more volatile in Table 7 than in Table 6, indicating that the difference in fixed transaction fees affects investor behavior. Lower fixed transaction fees make investors more willing to adjust their positions, while higher fixed transaction fees discourage trading activities. Since fixed transaction fees are related to the number of trades rather than the amount, higher fixed transaction fees have a particularly significant impact on small traders, who tend to maintain their existing positions and trade less frequently. In contrast, proportional transaction fees are linked to the amount invested, leading to different behavioral changes. Thus, even though transaction costs are proportionally the same, lower fixed fees in Table 7 prompt more trading, while higher fixed fees in Table 6 dampen willingness to trade.

5. Conclusions

Based on the results of the model analysis in this paper, this study reveals the significant impact of transaction costs (including proportional transaction fees and fixed transaction fees) on the optimization of blockchain asset portfolios. The findings show that regardless of whether the transaction costs are proportional or fixed, higher transaction costs widen the no-trade interval and reduce the frequency of investor trades, while lower transaction costs stimulate more trading behavior, as indicated by the increased trading activity observed in the lower transaction fee scenario.

For blockchain real estate token investments, both proportional and fixed transaction fees are prevalent, and this study highlights the importance of fully considering the difference in transaction fees for buying and selling when optimizing portfolio strategies. The study finds that in higher transaction cost environments, investors tend to adjust their portfolios less frequently, resulting in a more stable but less responsive asset allocation. In contrast, in a lower cost environment, investors tend to adjust their portfolios more dynamically in response to market changes.

Overall, transaction costs are a key factor in blockchain asset portfolio optimization. As the blockchain market continues to evolve with unique fee structures and volatility characteristics, investors must consider both proportional and fixed costs when constructing their portfolios. The model in this paper provides a valuable framework for analyzing different types of transaction costs and their impact on portfolio behavior, offering practical insights for investors seeking to optimize their portfolios in complex market environments.

Although our proposed multi-period portfolio optimization model effectively addresses key challenges related to proportional and fixed transaction costs in blockchain real estate token investments, certain limitations warrant further exploration. One major challenge lies in the fluctuating nature of real-world blockchain transaction fees, particularly gas fees, which are highly sensitive to network congestion and evolving protocol mechanisms. The assumption of constant transaction costs in our model simplifies these dynamics, and future research should incorporate a more adaptive framework that accounts for blockchain volatility and real-time network conditions. Additionally, while our model establishes theoretical scalability, practical implementation presents challenges. Currently, the framework is demonstrated using relatively small-scale portfolios, but extending it to large-scale, complex portfolios with numerous tokens and vast market data would significantly increase computational demands, potentially limiting its real-world applicability without further

methodological refinements.

Another key limitation is the lack of empirical validation with real-world trading data. While our numerical experiments provide theoretical insights into optimal trading strategies under different transaction cost scenarios, integrating historical blockchain transaction data would enhance the model's robustness and practical relevance. Future research could address these limitations by leveraging advanced machine learning techniques, such as reinforcement learning and deep neural networks, to dynamically optimize portfolio strategies in response to market fluctuations and transaction fee variations. Moreover, analyzing the influence of DeFi innovations—such as automated market makers, yield farming strategies, and decentralized lending protocols—could uncover new optimization opportunities within blockchain-based portfolio management. Furthermore, broadening the scope to account for blockchain-specific risks, including smart contract vulnerabilities and regulatory uncertainties, could enhance decision-making frameworks, making them more comprehensive and adaptable to real-world investment conditions.

Author contributions

Liyuan Zhang: Methodology and visualization; Limian Ci: Formal analysis; Yonghong Wu: Conceptualization and supervision; Benchawan Wiwatanapataphee: Supervision and validation. All authors have read and agreed to the published version of the manuscript.

Use of Generative-AI tools declaration

The authors declare they have not used Artificial Intelligence (AI) tools in the creation of this article.

Conflict of interest

The authors declare that there is no conflict of interest.

Prof. Benchawan Wiwatanapataphee is the Guest Editor of special issue "Innovative Advances in Mathematical Modeling and Simulation of Complex Systems" for AIMS Mathematics. Prof. Benchawan Wiwatanapataphee was not involved in the editorial review and the decision to publish this article.

References

1. H. Markowitz, Portfolio selection, *J. Financ.,* **7** (1952), 77–91. https://doi.org/10.1111/j.1540-6261.1952.tb01525.x
2. R. C. Merton, *Optimum consumption and portfolio rules in a continuous-time model*, In: Stochastic Optimization Models in Finance, Academic Press, New York, 1975, 621–661. https://doi.org/10.1016/B978-0-12-780850-5.50052-6
3. Z. Li, Y. Xu, Z. Du, Valuing financial data: The case of analyst forecasts, *Financ. Res. Lett.,* **75** (2025). https://doi.org/10.1016/j.frl.2025.106847
4. D. Amaya, G. Gauthier, T. O. Léautier, Dynamic risk management: Investment, capital structure, and hedging in the presence of financial frictions, *J. Risk Insur.,* **82** (2015), 359–399. https://doi.org/10.1111/jori.12025

5. C. Zheng, M. M. Chowdhury, A. D. Gupta, Investigating the influence of ownership on the relationship between bank capital and the cost of financial intermediation, *Data Sci. Financ. Econ.*, **4** (2024), 388–421. https://doi.org/10.3934/DSFE.2024017
6. M. J. P. Magill, G. M. Constantinides, Portfolio selection with transactions costs, *J. Econ. Theory,* **13** (1976), 245–263.
7. P. P. Boyle, T. Vorst, Option replication in discrete time with transaction costs, *J. Financ.,* **47** (1992), 271–293. https://doi.org/10.2307/2329098
8. Y. H. Fu, K. M. Ng, B. Huang, H. C. Huang, Portfolio optimization with transaction costs: A two-period mean-variance model, *Ann. Oper. Res.,* **233** (2015), 135–156. https://doi.org/10.1007/s10479-014-1574-x
9. M. S. Lobo, M. Fazel, S. Boyd, Portfolio optimization with linear and fixed transaction costs, *Ann. Oper. Res.,* **152** (2007), 341–365. https://doi.org/10.1007/s10479-006-0145-1
10. A. Kapteyn, F. Teppa, Subjective measures of risk aversion, fixed costs, and portfolio choice, *J. Econ. Psychol.,* **32** (2011), 564–580. https://doi.org/10.1016/j.joep.2011.04.002
11. L. Ante, Non-fungible token (NFT) markets on the Ethereum blockchain: Temporal development, cointegration and interrelations, *Econ. Innov. New Tech.,* **32** (2023), 1216–1234. https://doi.org/10.1080/10438599.2022.2119564
12. B. Biais, C. Bisiere, M. Bouvard, C. Casamatta, The blockchain folk theorem, *Rev. Financ. Stud.,* **32** (2019), 1662–1715. https://doi.org/10.1093/rfs/hhy095
13. Y. Lv, Transitioning to sustainable energy: Opportunities, challenges, and the potential of blockchain technology, *Front. Energy Res.,* **11** (2023), 1258044. https://doi.org/10.3389/fenrg.2023.1258044
14. D. Shang, Z. Yan, L. Zhang, Z. Cui, Digital financial asset price fluctuation forecasting in digital economy era using blockchain information: A reconstructed dynamic-bound Levenberg-Marquardt neural-network approach, *Expert Syst. Appl.,* **228** (2023), 120329. https://doi.org/10.1016/j.eswa.2023.120329
15. K. S. Chen, Interlinkages between Bitcoin, green financial assets, oil, and emerging stock markets, *Data Sci. Financ. Econ.,* **4** (2024), 160–187. https://doi.org/10.3934/DSFE.2024006
16. M. Aquilina, J. Frost, A. Schrimpf, Decentralized finance (DeFi): A functional approach, *J. Financ. Regul.,* **10** (2024), 1–27. https://doi.org/10.1093/jfr/fjad013
17. J. Meyn, M. Kandziora, S. Albers, M. Clement, Consequences of platforms' remuneration models for digital content: Initial evidence and a research agenda for streaming services, *J. Acad. Market. Sci.,* **51** (2023), 114–131. https://doi.org/10.1007/s11747-022-00875-6
18. A. Donmez, A. Karaivanov, Transaction fee economics in the Ethereum blockchain, *Econ. Inq.,* **60** (2022), 265–292. https://doi.org/10.1111/ecin.13020
19. Z. Y. Wang, M. Y. Li, J. Lu, X. Cheng, Business innovation based on artificial intelligence and blockchain technology, *Inform. Process. Manag.,* **59** (2022), 102759. https://doi.org/10.1016/j.ipm.2021.102759
20. M. Zheng, P. Sandner, *Asset tokenization of real estate in Europe*, In: Blockchains and the Token Economy: Theory and Practice, Springer, 2022, 179–211.
21. J. Schwiderowski, A. B. Pedersen, R. Beck, Crypto tokens and token systems, *Inform. Syst. Front.,* **26** (2024), 319–332. https://doi.org/10.1007/s10796-023-10382-w

22. H. E. Leland, Option pricing and replication with transactions costs, *J. Financ.,* **40** (1985), 1283–1301. https://doi.org/10.1111/j.1540-6261.1985.tb02383.x
23. M. H. A. Davis, A. R. Norman, Portfolio selection with transaction costs, *Math. Oper. Res.,* **15** (1990), 676–713. https://doi.org/10.1287/moor.15.4.676
24. X. L. Mei, F. J. Nogales, Portfolio selection with proportional transaction costs and predictability, *J. Bank. Financ.,* **94** (2018), 131–151. https://doi.org/10.1016/j.jbankfin.2018.07.012
25. B. Dumas, E. Luciano, An exact solution to a dynamic portfolio choice problem under transactions costs, *J. Financ.,* **46** (1991), 577–595. https://doi.org/10.1111/j.1540-6261.1991.tb02675.x
26. T. U. Gang, J. H. Choi, Optimal investment in an illiquid market with search frictions and transaction costs, *Appl. Math. Opt.,* **88** (2023), 3. https://doi.org/10.1007/s00245-023-09971-7
27. Z. Wang, S. Liu, Multi-period mean-variance portfolio selection with fixed and proportional transaction costs, *J. Ind. Manag. Optim.,* **9** (2013).
28. D. B. Brown, J. E. Smith, Dynamic portfolio optimization with transaction costs: Heuristics and dual bounds, *Manag. Sci.,* **57** (2011), 1752–1770. https://doi.org/10.1287/mnsc.1110.1377
29. S. Christensen, A. Irle, A. Ludwig, Optimal portfolio selection under vanishing fixed transaction costs, *Adv. Appl. Probab.,* **49** (2017), 1116–1143. https://doi.org/10.1017/apr.2017.36
30. S. Jiang, Y. Li, Q. Lu, Y. Hong, D. Guan, Y. Xiong, et al., Policy assessments for the carbon emission flows and sustainability of Bitcoin blockchain operation in China, *Nat. Commun.,* **12** (2021), 1–10.
31. Y. Leung, J. Wang, Minimax and biobjective portfolio selection based on collaborative neurodynamic optimization, *IEEE T. Neur. Net. Lear.*, **31** (2020), 2256–2267. https://doi.org/10.1109/TNNLS.2019.2950172
32. Y. Cai, K. L. Judd, R. Xu, *Numerical solution of dynamic portfolio optimization with transaction costs*, Working Paper, In: National Bureau of Economic Research, 2013. Available from: `https://www.nber.org/papers/w19132`.
33. P. Boyle, X. Lin, Optimal portfolio selection with transaction costs, *N. Am. Actuar. J.,* **1** (1997), 27–39. https://doi.org/10.1080/10920277.1997.10595602
34. *Commonwealth Bank of Australia, Term Deposit Interest Rates*, Commonwealth Bank. Available from: `https://www.commbank.com.au/personal/apply-online/download-printed-forms/InvInterestRates_ADB1072.pdf`.
35. L. Zhang, L. Ci, Y. Wu, B. Wiwatanapataphee, The real estate time-stamping and registration system based on Ethereum blockchain, *Blockchain Res. Appl.,* **5** (2024), 100175. https://doi.org/10.1016/j.bcra.2024.100175
36. *Australian Bureau of Statistics, Average Weekly Earnings, Australia: Latest Release*, Australian Bureau of Statistics, 2024. Available from: `https://www.abs.gov.au/statistics/labour/earnings-and-working-conditions/average-weekly-earnings-australia/latest-release`.

AIMS Press